



Cite this: DOI: 10.1039/c9nj04673a

Zn(II)@TFP-DAQ COF: an efficient mesoporous catalyst for the synthesis of *N*-methylated amine and carbamate through chemical fixation of CO₂†

 Priyanka Sarkar,^a Arpita Hazra Chowdhury,^a Sk. Riyajuddin,^b Surajit Biswas,^a Kaushik Ghosh^b and Sk. Manirul Islam^b *^a

Selective *N*-methylation and carbamate formation reactions were demonstrated via the chemical incorporation of CO₂ using a Zn-loaded TFP-DAQ COF (covalent organic framework) as an active catalyst under mild reaction conditions. The selective *N*-methylation and *N*-formylation reactions were performed by simply varying the type of solvent. The Zn(II)@TFP-DAQ COF catalyst was characterized via different characterization techniques such as PXRD, FTIR, UV-vis, N₂ adsorption–desorption studies, FESEM and TEM. The catalyst material showed pores in the mesoporous region with a high surface area of 1117.375 m² g⁻¹. The as-synthesized material was applied as a cheap catalyst for the *N*-methylation of secondary amines and in carbamate formation reactions with high yields of the desired products up to 98.5% and 97%, respectively, with >99% selectivity. The catalyst was found to be completely heterogeneous and reusable for multiple reaction cycles.

 Received 11th September 2019,
Accepted 28th November 2019

DOI: 10.1039/c9nj04673a

rsc.li/njc

1. Introduction

The removal of primary greenhouse gas carbon dioxide (CO₂) to valuable fine chemicals is very important for environmental remediation as the continuous accumulation of CO₂ in the atmosphere is the major cause of the global environmental problem worldwide.¹ Therefore, CO₂ capture and storage (CCS) have turned out to be a promising and fast-growing research topic for the depletion of the CO₂ emissions from flue gasses. CO₂ is an easily available and essential component in the global carbon cycle as well as non-toxic, non-flammable, renewable, and a low-cost C1 source, and it has great potential value as a C1 building block for C–C and C–N bond formations.² The synthesis of fine chemicals by CO₂ capture and conversion could have a major encouraging influence on the worldwide carbon balance.² There are several high surface area porous materials that support metallic nanoparticles and metal oxides³ as well as metal–organic frameworks (MOFs) containing multi-carboxylate linkers,⁴ which were reported as reusable heterogeneous catalysts for CO₂ fixation reactions for the large scale production of natural products, agrochemicals, fuels, and pharmaceutical compounds.

Covalent organic frameworks (COFs) are new-age materials, which are immaculate sets of covalently linked periodically ordered crystalline porous two-dimensional (2D) materials having a predictable network of molecular building blocks.⁵ The shape of a crystallite plays an important role in molecular adsorption,⁶ heterogeneous catalysis,⁷ CO₂ capture and conversion, sensing of metal-ions/molecules,⁸ gas separation and gas adsorption,⁹ light-harvesting,^{10a} pharmaceuticals^{10b} and as super-capacitors,¹¹ due to their embedded porosity, crystallinity, and a highly ordered and low density framework with highly accessible BET surface area and thermal stability.

As COFs show high CO₂ adsorption capacity, one of the promising routes for CO₂ utilisation is the synthesis of *N*-substituted compounds (*e.g.*, formamides, carbamates, and methylamines) via the C–N bond formation from amines under mild conditions, preferably at atmospheric pressure (CO₂) and low temperature; however, this is more difficult and challenging because CO₂ is thermodynamically stable and kinetically inert.¹² Carbamates and *N*-methylamines are widely used as intermediates for the synthesis of organic dyes, medicines, fragrances, and for the protection of the amine group.¹³ Usually, for the synthesis of formamides and methylamine from CO₂ and amines with H₂ over metal-based catalysts, high temperatures (> 100 °C) and/or high pressures (0.5–5 MPa) are required. However, in our experiment, instead of H₂, polymethylhydrosiloxane (PMHS) was used as the reductant since the polar Si–H bond with a mild reduction potential is kinetically more reactive than the H–H bond, which allows milder

^a Department of Chemistry, University of Kalyani, Kalyani, Nadia, 741235, W.B., India. E-mail: manir65@rediffmail.com; Fax: +91-33-2582-8282; Tel: +91-33-2582-8750

^b Institute of Nano Science and Technology, Mohali, 160062, India

† Electronic supplementary information (ESI) available. See DOI: 10.1039/c9nj04673a

reaction conditions,¹⁴ and it is cheap, non-toxic, easy-to-handle and can be easily removed from the reaction.¹⁵

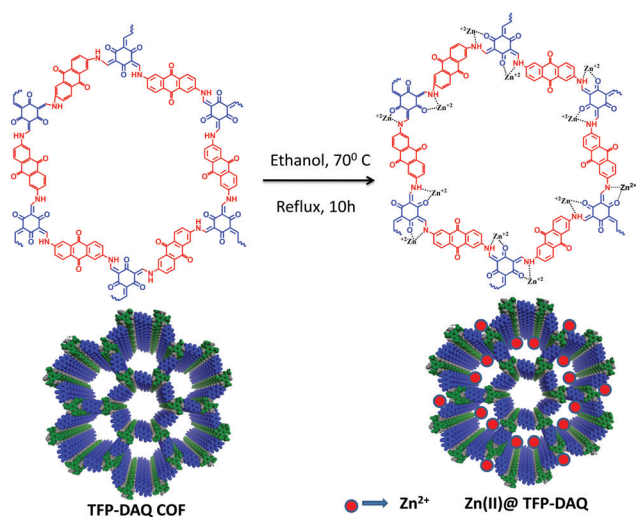
However, to date, there is little substrate scope mainly for methylation, most probably due to the difficulty in obtaining selectivity in methylation reactions, as formylation and methylation take place in the same system. Identifying catalytic systems with unique selective conditions for the two reactions appears to be a key challenge. Moreover, for this, the development of efficient, non-toxic, and recoverable catalytic systems for the transformation of CO₂ to *N*-substituted compounds is highly desirable.

Herein, we have developed an efficient Zn-based COF (Zn(II)@TFP-DAQ) heterogeneous catalyst, and we have represented a new methodology using the Zn(II)@TFP-DAQ catalyst for the construction of C–N bonds from CO₂ and amines to synthesize *N*-methylated amines and carbamate products under mild conditions. Amusingly, the Zn(II)@TFP-DAQ catalyst exhibited outstanding selectivity for both the formylation and methylation of amines. The substrate scope covers numerous different nitrogenous substrates for the reactions with >99% selectivity. To the best of our knowledge, it is the first report on Zn(II)@TFP-DAQ COF as a catalyst utilized in these two CO₂ incorporation reactions.

2. Experimental

2.1. Synthetic procedure for Zn(II)@TFP-DAQ COF

Initially, 1 g of the as-synthesized TFP-DAQ COF and 0.1 g of anhydrous ZnCl₂ salt were taken in a 50 mL round bottom (RB) flask containing 25 mL ethanol. The RB flask was fitted with a condenser and a magnetic stirrer. The reaction was processed for 10 h at 70 °C temperature. Then, the resulting Zn-loaded TFP-DAQ COF, *i.e.*, Zn(II)@TFP-DAQ, was obtained through filtration and washing with ethanol to remove any unreacted ZnCl₂ and finally, it was vacuum dried for 12 h at room temperature (Scheme 1).



Scheme 1 Synthetic route of Zn(II)@TFP-DAQ COF.

2.2. Procedure of *N*-methylation using the porous Zn(II)@TFP-DAQ COF Catalyst

The *N*-methylation of the respective amine was performed with a mixture of 2 mmol amines, PMHS (2 equiv.), 5 mL of solvent and 15 mg of the Zn(II)@TFP-DAQ COF catalyst. The reaction was processed in the presence of CO₂ (1 atm) at 80 °C temperature for 16 h. The COF catalyst was separated *via* filtration, and the organic filtrate was washed using a saturated NaHCO₃ solution, followed by drying over anhydrous Na₂SO₄. The yield of the preferred *N*-methylated product was analyzed *via* ¹HNMR spectroscopy.

2.3. Procedure carbamate synthesis using the porous Zn(II)@TFP-DAQ COF catalyst

Carbamate synthesis from aniline (2 mmol) and *n*-butyl bromide (2 mmol) was processed under a CO₂ atmosphere at room temperature for 8 h utilizing 20 mg Zn(II)@TFP-DAQ COF as the catalyst, and 10 mL DMSO as the solvent. After the completion of the reaction, the catalyst was separated and the organic portion was collected. The yield of the carbamate product was analyzed *via* ¹HNMR spectroscopy.

3. Results and discussion

3.1. Characterization

3.1.1. Powder X-ray diffraction (PXRD) analysis. The production of TFP-DAQ COF was established *via* the PXRD analysis, as depicted in Fig. 1. The characteristic peaks present at 3.6 and 27.2 correspond to the (100) and (001) diffraction planes, respectively. The peak at 27.1° arises from the π - π stacking of the (001) plane.¹⁶ The PXRD pattern of Zn(II)@TFP-DAQ COF was similar to that of the AA-eclipsed stacking model, and this results matched with a previously reported literature.¹⁶

3.1.2. FTIR analysis. The FTIR spectra of TFP, DAQ, TFP-DAQ COF, and Zn(II)@TFP-DAQ COF catalyst are shown in Fig. S1 (ESI†). The peaks at ~1266 cm⁻¹ and ~1554 cm⁻¹ are ascribed to the –(C–N) and –(C=C) bonds. The peaks in the FTIR spectra of DAQ in the range of 3418–3200 cm⁻¹ correspond to the –(N–H) bonds, which completely disappeared

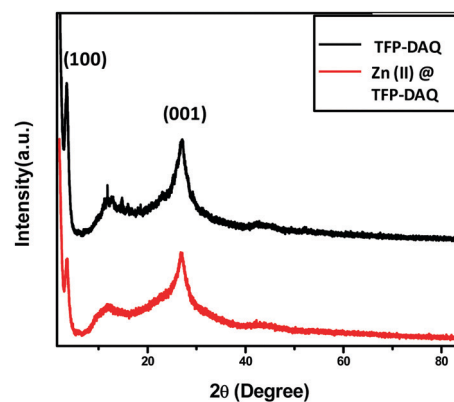


Fig. 1 Powder XRD patterns of the TFP-DAQ COF and Zn(II)@TFP-DAQ COF samples.

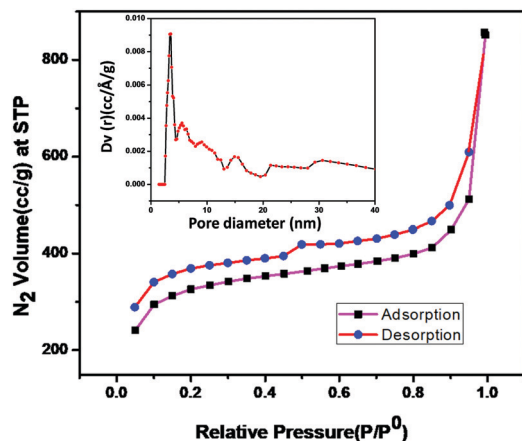


Fig. 2 N_2 adsorption-desorption isotherm of $Zn(II)$ @TFP-DAQ COF at 77 K. Pore size distribution plot (inset).

in the FTIR spectra of TFP-DAQ COF, thus confirming the complex formation between TFP and DAQ. The sharp peak at 1609 cm^{-1} in the spectra of TFP-DAQ COF is ascribed to the $-(C=O)$ bonds. The disappearance of the 1609 cm^{-1} peak in the spectra of $Zn(II)$ @TFP-DAQ COF catalyst indicates the coordination of $-(C=O)$ to the Zn metal.

3.1.3. UV-vis analysis. Fig. S2 (ESI†) illustrates the solid-state UV-visible absorbance spectra of the TFP-DAQ COF and $Zn(II)$ @TFP-DAQ COF catalysts. Both the materials showed broad absorption spectra in the range from 200 to 460 nm with a shoulder band at 490 nm. The absorption spectra include many transitions in the highly ordered conjugation systems.¹⁷

3.1.4. Surface area measurement. The N_2 adsorption-desorption isotherms of the $Zn(II)$ @TFP-DAQ COF catalyst is depicted in Fig. 2. The subsequent pore size distribution (PSD) resulting from the respective desorption data is given in the index of the respective isotherm plot. The $Zn(II)$ @TFP-DAQ COF catalyst has a narrow peak at the 3.5 nm pore diameter and has some broad peaks of pores in the range from 4.6 nm to 35 nm, which confirms the mesoporous nature of the catalyst. The mean pore size was found to be 14.8 nm. The estimated BET surface area and total pore volume of the $Zn(II)$ @TFP-DAQ COF were observed to be $1117.375\text{ m}^2\text{ g}^{-1}$ and $1.31\text{ cm}^3\text{ g}^{-1}$, respectively.

3.1.5. Microscopic analysis. The FESEM images (Fig. 3) of the TFP-DAQ COF (Fig. 3a and b) and $Zn(II)$ @TFP-DAQ COF (Fig. 3c and d) samples show the disordered fibrous morphology.

The elemental mapping images of carbon, nitrogen, oxygen, and Zn of the catalyst material are shown in Fig. 4a-e. The interparticle porosity of the mesoporous COF material is confirmed by the TEM images (Fig. 5a and b). The elemental composition of the TFP-DAQ COF and $Zn(II)$ @TFP-DAQ COF materials are confirmed by the EDAX patterns (Fig. 6a and b) of the materials.

3.1.6. XPS analysis. Fig. 7 shows the XPS spectra of Zn in the catalyst sample, where the Zn $2p_{3/2}$ and Zn $2p_{1/2}$ peaks appeared at 1022.1 eV and 1045.1 eV, respectively. The spin-orbit

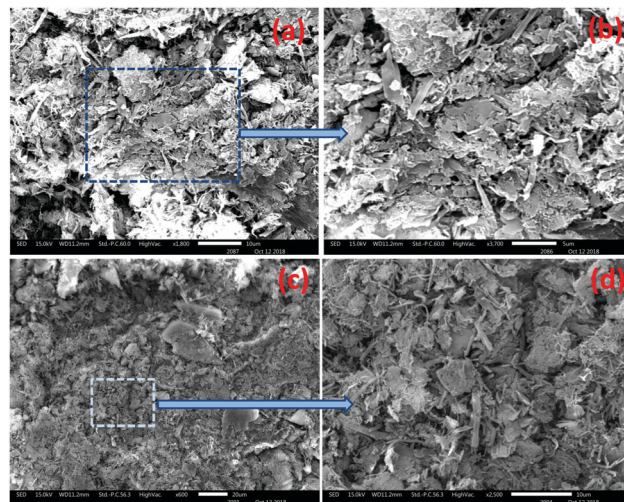


Fig. 3 FE-SEM images of the TFP-DAQ COF (a and b) and $Zn(II)$ @TFP-DAQ COF (c and d) samples at different magnifications.

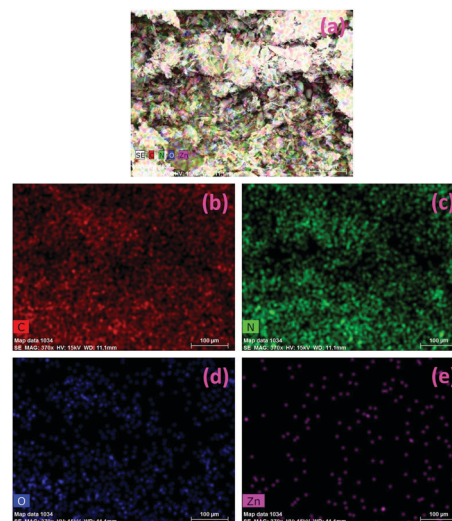


Fig. 4 EDS mapping images of $Zn(II)$ @TFP-DAQ COF: (a) electron microscopic image, C (b), N (c), O (d), Zn (e) element EDS mapping.

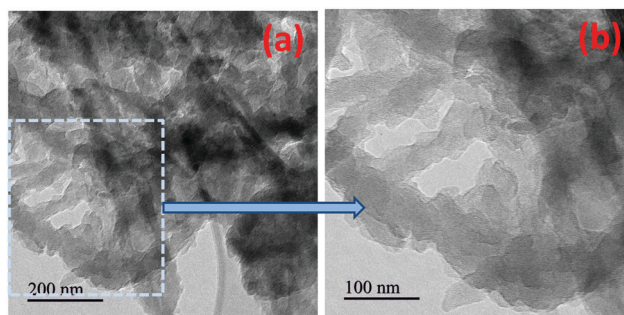


Fig. 5 TEM images of $Zn(II)$ @TFP-DAQ COF sample.

splitting distance at 23 eV indicated the Zn presence in the catalyst system as the Zn^{+2} state.¹⁸

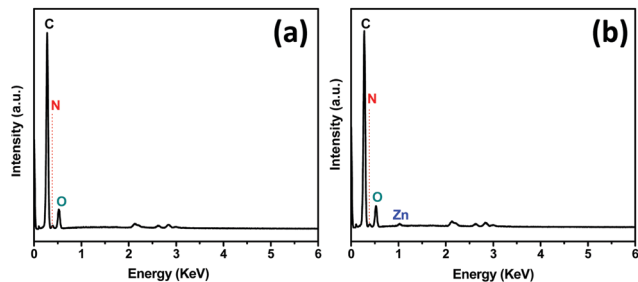


Fig. 6 EDAX pattern of the TFP-DAQ COF (a) and Zn(II)@TFP-DAQ COF (b) samples.

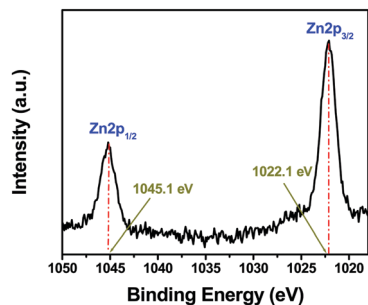


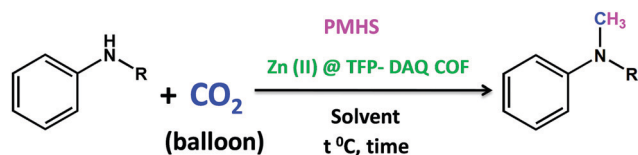
Fig. 7 XPS spectra of Zn 2p peak of Zn(II)@TFP-DAQ COF.

3.2. Catalytic activity

3.2.1. *N*-Methylation of amines catalyzed by the Zn(II)@TFP-DAQ COF. The chemical fixation of CO₂ via the *N*-methylation of amine over the mesoporous Zn(II)@TFP-DAQ COF catalyst in the presence of hydrosilane under 1 atmospheric pressure of CO₂ at 80 °C temperature is depicted in Scheme 2.

The yield of the preferred product was optimized using different kinds of solvents and varying the reaction temperature (Table 1). Both of the factors showed a noticeable effect on the product yield. The probable side product of this *N*-methylation reaction is the *N*-formylated amine (Scheme 3B). Therefore, we have studied the selectivity of the methylation reaction.

The *N*-methylation reaction was studied in the presence of different solvents and different reaction temperatures (Table 1). Therefore, we have used different kinds of solvents, such as acetonitrile, 1,4-dioxane, THF, DMF, and toluene, to increase the yield of the product. Among the used solvents, acetonitrile was found to be the most efficient solvent for the synthesis of the *N*-methylated product with a high yield of >99% (Table 1, entry 1). 1,4-Dioxane also showed a high yield of the *N*-methylated product (Table 1, entry 2). Moreover, in the presence of THF as a solvent, the

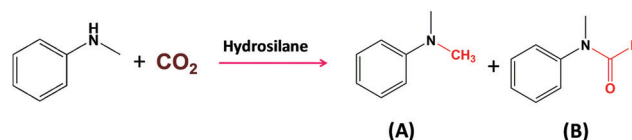


Scheme 2 *N*-Methylation of amines through the chemical fixation of CO₂.

Table 1 Effect of solvent and temperature on the *N*-methylation of *N*-methyl aniline^a

Entry	Solvent	Temperature (°C)	Yield ^b (%) (A) [selectivity (%)]	Yield ^b (%) (B) [selectivity (%)]
1	Acetonitrile	80	>99 [>99]	—
2	1,4-Dioxane	80	98.5 [>99]	—
3	THF	80	—	>98 [>99]
4	Toluene	80	—	—
5	DMF	80	—	—
6	Acetonitrile	50	57 [>99]	—
7	Acetonitrile	r.t.	11 [>99]	—
8 ^c	—	80	—	—

^a Reactions performed at atmospheric pressure (1 atm) of CO₂ using *N*-methyl aniline (2.0 mmol), Zn(II)@TFP-DAQ COF catalyst (15 mg), PMHS (2 equiv.), solvent (5 mL), 16 h. ^b GC yield. ^c Without solvent.



Scheme 3 Probable products of the *N*-methylation reaction of *N*-methyl aniline.

reaction showed *N*-formylated product as the major product, with a high yield (Table 1, entry 3). Interestingly, in the presence of different solvents, either the *N*-methylated or the *N*-formylated products was obtained with high selectivity (>99%). In the presence of toluene and DMF, there was no reaction even at high temperatures (Table 1, entries 4 and 5). At room temperature, in the presence of acetonitrile, only 11% product yield of the *N*-methylated product was found (Table 1, entry 7). With the increase in temperature, the product yield was also increased and the highest yield was obtained at 80 °C temperature (Table 1, entry 1). It is very important to note that the selectivity of the desired products was always maintained >99% for all the reactions studied to optimize the reaction. There was no product found in the absence of any solvent, even at 80 °C temperature (Table 1, entry 8).

The reaction was also standardized by varying the catalyst loading and amount of PMHS (Table 2). The amount of PMHS was varied from 0.5 equiv. to 2 equiv. (Table 2, entries 1–3).

Table 2 Effect of catalyst loading and the amount of PMHS on the *N*-methylation of *N*-methyl aniline^a

Entry	Catalyst loading (mg)	Amount of PMHS (equiv.)	Yield ^b (%) (A)	Yield ^b (%) (B)
1	15	0.5	Trace	—
2	15	1	25	—
3	15	2	>99	—
4	10	2	53	—
5	5	2	23	—
6 ^c	—	2	—	—
7 ^d	15	—	—	—

^a Reactions performed at atmospheric pressure (1 atm) of CO₂ using *N*-methyl aniline (2.0 mmol), Zn(II)@TFP-DAQ COF catalyst, PMHS, 80 °C, 16 h, acetonitrile (5 mL). ^b GC yield. ^c Without catalyst. ^d Without PMHS.

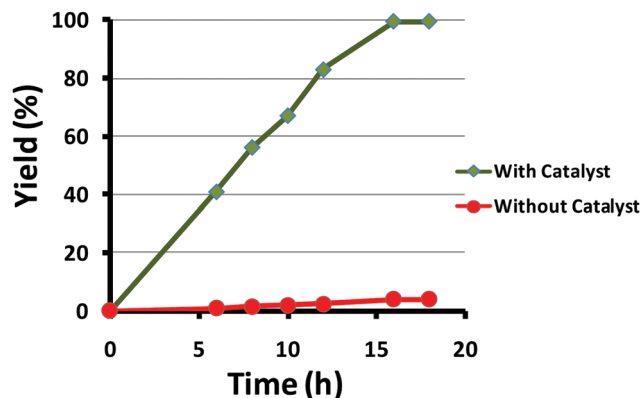


Fig. 8 Reaction rate study in the presence and in the absence of the catalyst.

By using 1 equiv. of PMHS, only 25% of the methylated product was obtained (Table 2, entry 2), and the yield excellently increased to >99% when using 2 equiv. of PMHS (Table 2, entry 3). With the increase in the amount of the catalyst loading from 5 mg to 15 mg, the methylated product yield also increased from 23% to >99% (Table 2, entries 3–5). No product was obtained in the absence of a catalyst (Table 2, entry 6) and also, no reaction occurred in the absence of PMHS (Table 2, entry 7).

We have studied the reaction rates with time in the presence as well as in the absence of the $\text{Zn(II)}@TFP\text{-DAQ}$ COF catalyst (Fig. 8). It was clearly observed that when the reaction was performed in the presence of the catalyst, the reaction rate sharply increased with a high slope of the curve and finished within 16 h. However, when the reaction was performed in the absence of the catalyst, a very slow increase in the reaction rate was observed, and a yield of <5% was found even after 18 h of reaction time.

The *N*-methylation reaction was performed on several types of secondary amines (2 mmol) using 15 mg of the $\text{Zn(II)}@TFP\text{-DAQ}$

Table 3 *N*-Methylation catalysed by $\text{Zn(II)}@TFP\text{-DAQ}$ COF^a

Entry	Amine	Product	Yield ^b (%)	TON	TOF (h ⁻¹)
1			98.5	4.86×10^2	30.4
2			93	4.59×10^2	28.7
3			94	4.64×10^2	29.0
4			96	4.74×10^2	29.6
5			83	4.10×10^2	25.6

^a Reactions performed at atmospheric pressure (1 atm) of CO_2 using *N*-methylaniline (2.0 mmol), $\text{Zn(II)}@TFP\text{-DAQ}$ COF catalyst (15 mg), PMHS (2 equiv.), 80 °C, 16 h, acetonitrile (5 mL). ^b Isolated yield.

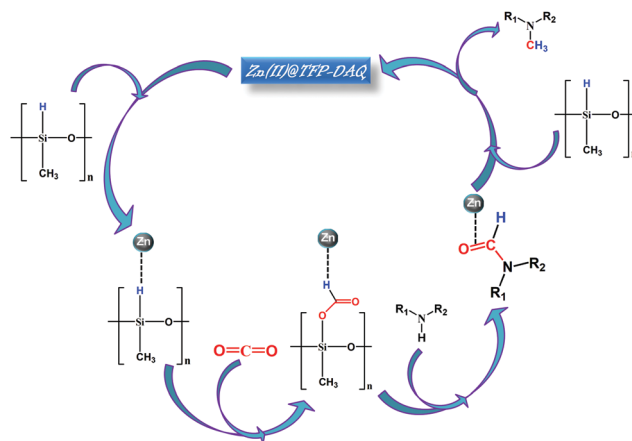


Fig. 9 Proposed mechanistic pathway for the *N*-methylation of amine over the $\text{Zn(II)}@TFP\text{-DAQ}$ COF catalyst.

COF catalyst, 2 equiv. of PMHS under CO_2 balloon at 80 °C temperature in the presence of acetonitrile. Most of the secondary amines showed excellent yield (>90%) of the corresponding *N*-methylated products (Table 3, entries 1–4) except *N*-phenylbenzylamine, which showed a slightly poor yield (83%) (Table 3, entry 5) and that could be due to the steric hindrance of the bulky benzyl group.

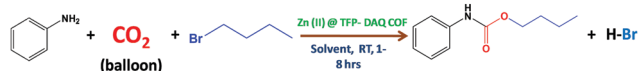
The probable mechanistic route^{19,20} for the synthesis of *N*-methyl amine *via* CO_2 incorporation over the $\text{Zn(II)}@TFP\text{-DAQ}$ COF catalyst is shown in Fig. 9. The *N*-methylated product was obtained, when the Zn metal activated the Si–H bond of hydrosiloxane (PMHS), followed by the CO_2 incorporation into the Si–H bond. As PMHS has multiple Si–H bonds, it effectively supplies hydrogen to the reaction system for the carbonyl group reduction to obtain the *N*-methylated amine.

3.2.2. Alkyl and aryl carbamate synthesis catalyzed by $\text{Zn(II)}@TFP\text{-DAQ}$ COF. The mesoporous $\text{Zn(II)}@TFP\text{-DAQ}$ COF material was used as a catalyst for the carbamate synthesis reaction (Scheme 4) in the absence of any base and temperature.

The reaction condition was optimized using the synthetic procedure of butyl *N*-phenyl carbamate (Scheme 5). The effect of parameters, such as reaction time (Table 4, entries 1–4) and different solvents (Table 4, entries 4–6), were studied. Among the solvents, DMSO and DMF (Table 4, entries 4 and 5) showed a better yield of the needed carbamate product than toluene (Table 4, entry 6). DMSO showed the best yield of the product. Therefore, we have chosen DMSO as the reaction solvent for the



Scheme 4 Synthesis of carbamates through the chemical fixation of CO_2 .

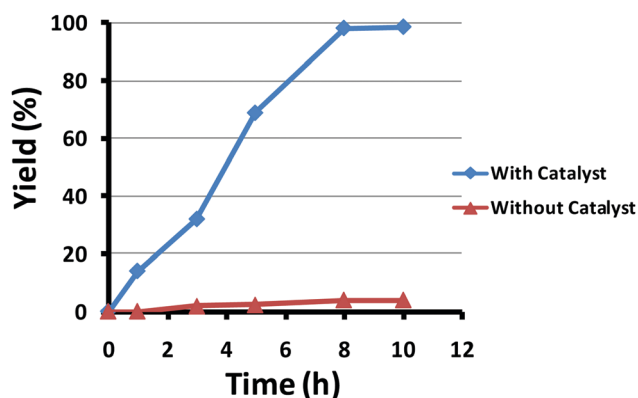


Scheme 5 Butyl *N*-phenyl carbamate synthesis *via* CO_2 incorporation.

Table 4 Effect of solvent and reaction time on carbamate synthesis reaction^a

Entry	Solvent	Reaction time (h)	Yield ^b (%) [selectivity (%)]
1	DMSO	1	14 [>99]
2	DMSO	3	32 [>99]
3	DMSO	5	69 [>99]
4	DMSO	8	98 [>99]
5	DMF	8	85 [>99]
6	Toluene	8	72 [>99]
7 ^c	—	8	32 [>99]

^a Reactions performed under CO₂ (1 atm) at room temperature using 20 mg of catalyst, 2 mmol amine, 2 mmol of alkyl/aryl bromide and 10 mL solvent. ^b GC yield of carbamate. ^c Without solvent.

**Fig. 10** Reaction rate study in the presence and in the absence of the catalyst.

carbamate synthesis reaction. In the absence of any solvent, only 32% of the product was obtained (Table 4, entry 7). In the presence of DMSO as the solvent, it was interesting to note that with an increase in the reaction time from 1 h to 8 h, the yield of the product also increased from 14% to 98% (Table 4, entries 1–4).

We have studied the reaction rates with time in the presence as well as in the absence of Zn(II)@TFP-DAQ COF catalyst (Fig. 10). It was clearly observed that when the reaction was carried out in the presence of the catalyst, the reaction rate sharply increased with a high slope of the curve and finished within 8 h. However, when the reaction was performed in the absence of the catalyst, a very slow increase in the reaction rate was observed and a yield of <5% was found even after 10 h of the reaction time.

The carbamate synthesis reaction was studied under an optimized reaction condition on aniline, *p*-anisidine, *p*-chloroaniline and *N*-methylaniline with butyl bromide and benzyl bromide (Table 5, entries 1–8). Aniline and *p*-chloroaniline showed a very good yield of the carbamate products with the alkyl bromide (Table 5, entries 1 and 3) as well as with the aryl bromide (Table 5, entries 5 and 7). Moreover, *p*-anisidine and *N*-methylaniline showed a relatively poor yield of the carbamate products with the alkyl and aryl bromides (Table 5, entries 2, 4, 6 and 8).

3.3. Heterogeneity test

The Zn loading percentage (%) was studied in Zn(II)@TFP-DAQ COF *via* atomic absorption spectroscopy (AAS), which was

Table 5 Carbamate synthesis catalyzed by Zn(II)@TFP-DAQ COF^a

Entry	Amines	Bromide	Products	Yield ^b (%)	TON	TOF (h ⁻¹)
1				97	3.6×10^2	45.0
2				84	3.1×10^2	38.8
3				95	3.5×10^2	43.7
4				80	2.9×10^2	37.0
5				96	3.5×10^2	44.4
6				80	2.9×10^2	37.0
7				93	3.4×10^2	43.0
8				72	2.6×10^2	33.3

^a Reactions performed under CO₂ (1 atm) at room temperature using 20 mg of catalyst, 2 mmol amine, 2 mmol of alkyl/aryl bromide and 10 mL DMSO, 8 h. ^b Isolated yield of carbamate.

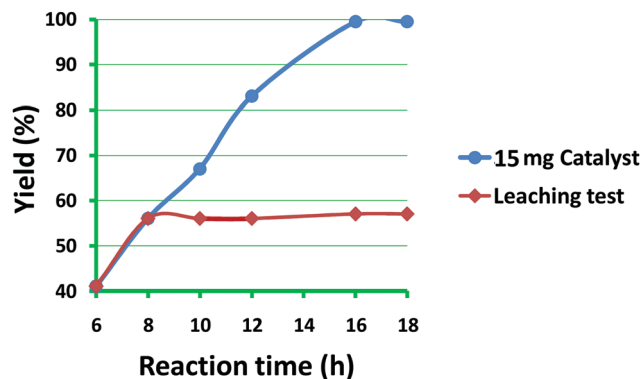


Fig. 11 Heterogeneity test suggesting the minimal leaching of the active metal into the filtrate solution.

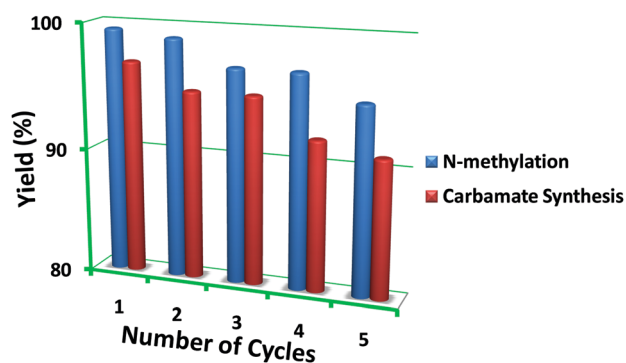


Fig. 12 Recyclability diagram of the mesoporous Zn(II)@TFP-DAQ COF catalyst.

observed to be 1.76%. The heterogeneous property of the Zn(II)@TFP-DAQ COF catalyst was studied *via* a hot filtration test. The test was conducted on the *N*-methylation reaction of *N*-methylaniline. After conducting the reaction for 8 h, a 56% yield was obtained. Then, the catalyst was isolated from the reaction mixture, and the reaction was conducted again in the absence of the catalyst for another 10 h. It was observed that the yield of the product remained the same (approximately 56%) after separating the catalyst (Fig. 11), which implied that there was no further reaction happening after isolating the catalyst. There was no leaching of the active metal found *via* the ICP-AES study of the filtrate, implying minimal zinc metal leaching from the porous TFP-DAQ COF support throughout the reaction, and

the Zn(II)@TFP-DAQ COF catalyst was completely heterogeneous in nature.

3.4. Recyclability of the Zn(II)@TFP-DAQ COF catalyst

One of the most important characteristics of heterogeneous catalysts is the recyclability of the material. We have checked the recyclability of the catalyst for five consecutive cycles for both the reactions *via* collecting the catalyst by centrifugation after completing each cycle. The result is shown in Fig. 12, which indicates that there was almost no considerable change in the yields of the products, suggesting no catalyst deactivation. The FESEM image of the reused catalyst (Fig. S3, ESI[†]) suggested that the catalyst retained its structural characteristics after recycling. We have also studied the structural details and pore structure of the reused catalyst after five reaction cycles *via* XRD (Fig. S4, ESI[†]) and nitrogen adsorption/desorption study (Fig. S5, ESI[†]). The XRD showed no considerable changes in the reused catalyst. The nitrogen adsorption/desorption study of the reused catalyst showed a decrease in the BET surface area (700.545 m² g⁻¹) with a relatively smaller pore size (3.2 nm) due to blocking of the pores because of the use of PMHS in the reaction. We have also done the EDS mappings (Fig. S6, ESI[†]) of the recovered catalyst, which showed the presence of silicon, suggesting the existence of a by-product derived from the PMHS on the catalyst surface. Furthermore, we have done the EDAX analysis of the reused catalyst, which also confirmed the presence of silicon from the PMHS in the reused catalyst (Fig. S7, ESI[†]).

From the comparative chart (Table 6), it can be clearly observed that the mesoporous Zn(II)@TFP-DAQ COF catalyst showed a relatively improved yield of the desired *N*-methylated and carbamate products with much higher TOF (h⁻¹) values than the other reported catalysts under 1 atmospheric pressure of CO₂.

4. Conclusions

A mesoporous Zn(II)@TFP-DAQ COF catalyst was synthesized with a high surface area. This cheap catalyst material showed efficient catalytic performance for CO₂ incorporation reactions such as the *N*-methylation of secondary amines and carbamate synthesis under atmospheric pressure of CO₂ with high yield as well as high selectivity of the needed products. In addition, the

Table 6 Comparison chart of the mesoporous Zn(II)@TFP-DAQ COF catalyst with other reported catalysts

Reaction	Catalyst	Reaction condition	Time (h)	Yield (%)/ TOF (h ⁻¹)	Ref.
<i>N</i> -Methylation	Rhodium perimidine-based NHC complex	<i>N</i> -Methyl aniline (0.5 mmol), PhSiH ₃ (2 mmol, 4 equiv.), catalyst (5 mol%), 90 °C, 2 mL toluene, 1 atm of CO ₂	16	> 98/24.5	21
	Mesoporous Zn(II)@TFP-DAQ COF	<i>N</i> -Methyl aniline (2 mmol), PMHS (2 equiv.), catalyst (15 mg), 80 °C, 5 mL, acetonitrile, 1 atm of CO ₂	16	98.5/30.4	This study
Carbamate synthesis	Zeolite-beta	Aniline (10 mmol), <i>n</i> -butyl bromide (10 mmol), catalyst (150 mg), CO ₂ (3.4 bar), 353 K	4	52.8/5.9	22
	Mesoporous Zn(II)@TFP-DAQ COF	Aniline (2 mmol), <i>n</i> -butyl bromide (2 mmol), catalyst (20 mg), 10 mL DMSO, RT, 1 atm of CO ₂	8	97/45.0	This study

reusability of the catalyst material was observed multiple times, signifying the mesoporous Zn(II)@TFP-DAQ COF material as a potentially active, new and cheap heterogeneous catalyst for CO₂ incorporation reactions.

Conflicts of interest

There are no conflicts to declare.

Acknowledgements

SMI is thankful to DST-SERB (project reference no. EMR/2016/004956), New Delhi, Govt. of India, Board of Research in Nuclear Sciences (BRNS), Govt. of India, Project reference no. 37(2)/14/03/2018-BRNS/37003, and Council of Scientific and Industrial and Research, CSIR (project reference no. 02(0284)2016/EMR-II dated 06/12/2016), New Delhi, Govt. of India for providing financial support. P. Sarkar is thankful to CSIR, New Delhi, Govt. of India, for her CSIR-JRF fellowship. A. Hazra Chowdhury is thankful to the University of Kalyani, India for providing her URS fellowship. S. Biswas acknowledges the University Grants Commission for his D. S. Kothari Post Doctoral Fellowship (Award letter no. F.4-2/2006 (BSR)/CH/16-17/0026). We acknowledge the Department of Science and Technology (DST) and University Grant Commission (UGC) New Delhi, India for providing support to the Department of Chemistry, the University of Kalyani under PURSE, FIST and SAP program.

Notes and references

- (a) B. Kumar, M. Llorente, J. Froehlich, T. Dang, A. Sathrum and C. P. Kubiak, *Annu. Rev. Phys. Chem.*, 2012, **63**, 541–569; (b) N. Armaroli and V. Balzani, *Angew. Chem., Int. Ed.*, 2007, **46**, 52–66; (c) W. Song, Z. Chen, M. K. Brennaman, J. J. Concepcion, A. O. T. Patrocínio, N. Y. M. Iha and T. J. Meyer, *Pure Appl. Chem.*, 2011, **83**, 749–768; (d) R. Quadrelli and S. Peterson, *Energy Policy*, 2007, **35**, 5938–5952; (e) Y. Z. Meng, L. C. Du, S. C. Tjong, Q. Zhu and A. S. Hay, *J. Polym. Sci., Part A: Polym. Chem.*, 2002, **40**, 3579–3591.
- (a) H.-H. Guan, H. Lei, M. Chen, Z.-H. Ren, Y. Bai and Y.-Y. Wang, *Adv. Synth. Catal.*, 2012, **354**, 489; (b) Q. Liu, L. Wu, R. Jackstell and M. Beller, *Nat. Commun.*, 2015, **6**, 5933; (c) M. Pera-Titus, *Chem. Rev.*, 2013, **114**, 1413; (d) G. Fiorani, W. Guo and A. W. Kleij, *Green Chem.*, 2015, **17**, 1375–1389; (e) Q. Liu, L. Wu, R. Jackstell and M. Beller, *Nat. Commun.*, 2015, **6**, 5933; (f) M. Aresta, A. Dibenedetto and A. Angelini, *Chem. Rev.*, 2014, **114**, 1709–1742; (g) A. Julián, V. Polo, E. A. Jaseer, F. J. Fernández-Alvarez and L. A. Oro, *ChemCatChem*, 2015, **7**, 3895–3902.
- P. Bhanja, A. Modak and A. Bhaumik, *Chem. – Eur. J.*, 2018, **24**, 7278–7297.
- S. K. Das, S. Chatterjee, S. Bhunia, A. Mondal, P. Mitra, V. Kumari, A. Pradhan and A. Bhaumik, *Dalton Trans.*, 2017, **46**, 13783–13792.
- (a) X. Han, Q. Xia, J. Huang, Y. Liu, C. Tan and Y. Cui, *J. Am. Chem. Soc.*, 2017, **139**, 8693; (b) S. F. Pang, S. Q. Xu, T. Y. Zhou, R. R. Liang, T. G. Zhan and X. Zhao, *J. Am. Chem. Soc.*, 2016, **138**, 4710; (c) Y. Zhang, J. Duan, D. Ma, P. Li, S. Li, H. Li, J. Zhou, X. Ma, X. Feng and B. Wang, *Angew. Chem., Int. Ed.*, 2017, **56**, 16313; (d) Q. Sun, B. Aguilá, J. Perman, L. D. Earl, C. W. Abney, Y. Cheng and S. Wei, *J. Am. Chem. Soc.*, 2017, **139**, 2786.
- (a) P. Borah, X. K. T. Nguyen and Y. L. Zhao, *Angew. Chem., Int. Ed.*, 2012, **51**, 7756; (b) S. Bhunia, B. Banerjee and A. Bhaumik, *Chem. Commun.*, 2015, **51**, 5020; (c) M. Rose, *ChemCatChem*, 2014, **6**, 1166; (d) P. Puthiaraj and K. Pitchumani, *Green Chem.*, 2014, **16**, 4223.
- (a) J. Yu and P. B. Balbuena, *J. Phys. Chem. C*, 2013, **117**, 3383; (b) A. P. Katsoulidis, S. M. Dyar, R. Carmieli, C. D. Malliakas, M. R. Wasielewski and M. G. Kanatzidis, *J. Mater. Chem. A*, 2013, **1**, 10465; (c) S. Lin, Y. Hou, X. Deng, H. Wang, S. Sun and X. Zhang, *RSC Adv.*, 2015, **5**, 41017–41024; (d) Y. Wu, H. Xu, X. Chen, J. Gao and D. Jiang, *Chem. Commun.*, 2015, **51**, 10096–10098; (e) V. S. Vyas, F. Haase, L. Stegbauer, G. Savasci, F. Podjaski, C. Ochsenfeld and B. V. Lotsch, *Nat. Commun.*, 2015, **6**, 8508.
- (a) G. Das, B. P. Biswal, S. Kandambeth, V. Venkatesh, G. Kaur, M. Addicoat, T. Heine, S. Verma and R. Banerjee, *Chem. Sci.*, 2015, **6**, 3931; (b) L. Hou, C. L. Zhu, X. P. Wu, G. N. Chen and D. P. Tang, *Chem. Commun.*, 2014, **50**, 1441; (c) T. A. Fayed, M. H. Shaaban, M. N. El-Nahass and F. M. Hassan, *Microporous Mesoporous Mater.*, 2014, **198**, 144.
- (a) H. Furukawa and O. M. Yaghi, *J. Am. Chem. Soc.*, 2009, **131**, 8875–8883; (b) Z. Li, Y. Zhi, X. Feng, X. Ding, Y. Zou, X. Liu and Y. Mu, *Chem. – Eur. J.*, 2015, **21**, 12079–12084; (c) S. Wu, S. Gu, A. Zhang, G. Yu, Z. Wang, J. Jianc and C. Pan, *J. Mater. Chem. A*, 2015, **3**, 878–885; (d) H. Takeda, M. Ohashi, Y. Goto, T. Ohsuna, T. Tani and S. Inagaki, *Chem. – Eur. J.*, 2014, **20**, 9130; (e) M. G. Rabbani, A. K. Sekizkardes, Z. Kahveci, T. E. Reich, R. Ding and H. M. El-Kaderi, *Chem. – Eur. J.*, 2013, **19**, 3324.
- (a) H. Takeda, M. Ohashi, Y. Goto, T. Ohsuna, T. Tani and S. Inagaki, *Chem. – Eur. J.*, 2014, **20**, 9130; (b) H. Y. Lian, M. Hu, C. H. Liu, Y. Yamauchi and K. C.-W. Wu, *Chem. Commun.*, 2012, **48**, 5151.
- (a) C. R. Mulzer, L. Shen, R. P. Bisbey, J. R. McKone, N. Zhang, H. D. Abruñ and W. R. Dichtel, *ACS Cent. Sci.*, 2016, **2**, 667–673; (b) A. M. Khattak, Z. A. Ghazi, B. Liang, N. A. Khan, A. Iqbal, L. Li and Z. Tang, *J. Mater. Chem. A*, 2016, **4**, 16312–16317.
- (a) R. H. Heyn, I. Jacobs and R. H. Carr, *Adv. Inorg. Chem.*, 2014, **66**, 83–115; (b) O. Kreye, H. Mutlu and M. A. R. Meier, *Green Chem.*, 2013, **15**, 1431–1455; (c) D. Chaturvedi, *Tetrahedron*, 2012, **68**, 15–45; (d) B. C. Chen, M. S. Bednarz, R. Zhao, J. E. Sundeen, P. Chen, Z. Shen, A. P. Skoumbourdis and J. C. Barrish, *Tetrahedron Lett.*, 2000, **41**, 5453; (e) A. Tlili, E. Blondiaux, X. Frogneux and T. Cantat, *Green Chem.*, 2015, **17**, 157.
- Q. Liu, L. Wu, R. Jackstell and M. Beller, *Nat. Commun.*, 2015, **6**, 5933.

- 14 (a) A. Tlili, E. Blondiaux, X. Frogneux and T. Cantat, *Green Chem.*, 2015, **17**, 157–168; (b) M. Liu, T. Qin, Q. Zhang, C. Fang, Y. Fu and B.-L. Lin, *Sci. China: Chem.*, 2015, **58**, 1524–1531.
- 15 (a) S. Zhou, K. Junge, D. Addis, S. Das and M. Beller, *Angew. Chem., Int. Ed.*, 2009, **48**, 9507; (b) S. Das, D. Addis, S. Zhou, K. Junge and M. Beller, *J. Am. Chem. Soc.*, 2010, **132**, 1770; (c) S. Das, D. Addis, K. Junge and M. Beller, *Chem. – Eur. J.*, 2011, **43**, 12186; (d) S. Das, B. Wendt, K. Möller, K. Junge and M. Beller, *Angew. Chem., Int. Ed.*, 2012, **51**, 1662; (e) S. Das, Y. Li, C. Bornschein, S. Pisiewicz, K. Kiersch, D. Michalik, F. Gallou, K. Junge and M. Beller, *Angew. Chem., Int. Ed.*, 2015, **54**, 12389; (f) S. Das, Y. Li, K. Junge and M. Beller, *Chem. Commun.*, 2012, **48**, 10742.
- 16 S. Karak, S. Kandambeth, B. P. Biswal, H. Sekhar Sasmal, S. Kumar, P. Pachfule and R. Banerjee, *J. Am. Chem. Soc.*, 2017, **139**, 1856–1862.
- 17 G.-H. Fan, X. Li, J.-Y. Liu and G.-Z. He, *Comput. Theor. Chem.*, 2014, **1030**, 17–24.
- 18 E. Olegario, C. M. Pelicano, J. C. Felizco and H. Mendoza, *Mater. Res. Express*, 2019, **6**, 085204.
- 19 A. H. Chowdhury, U. kayal, I. H. Chowdhury, S. Ghosh and S. M. Islam, *ChemistrySelect*, 2019, **4**, 1069–1077.
- 20 L. González-Sebastián, M. Flores-Alamo and J. J. García, *Organometallics*, 2015, **34**, 763–769.
- 21 R. H. Lam, C. M. A. McQueen, I. Pernik, R. T. McBurney, A. F. Hill and B. A. Messerle, *Green Chem.*, 2019, **21**, 538–549.
- 22 R. Srivastava, D. Srinivas and P. Ratnasamy, *Appl. Catal., A*, 2005, **289**, 128–134.